Pure Appl. Chem., Vol. 83, No. 1, pp. 1–8, 2011.
doi:10.1351/PAC-CON-10-08-10

Redox properties of CdSe and CdSe–ZnS quantum dots in solution*

Matteo Amelia[1], Tommaso Avellini[1], Simone Monaco[1], Stefania Impellizzeri[2], Ibrahim Yildiz[2], Françisco M. Raymo[2], and Alberto Credi[1,‡]

[1]Department of Chemistry "G. Ciamician", University of Bologna, via Selmi 2, 40126 Bologna, Italy; [2]Department of Chemistry, University of Miami, 1301 Memorial Drive, Coral Gables, FL 33146-0431, USA

Abstract: Semiconductor quantum dots (QDs) are inorganic nanoparticles which, because of their unique size-dependent electronic properties, are of high potential interest for the construction of functional nanodevices. Photoinduced electron transfer is a versatile mechanism used to implement light-induced functionalities in multicomponent (supra)molecular assemblies. Indeed, QDs can be employed as active components in new generations of these systems. The rational design of the latter, however, requires prior knowledge of the photophysical properties and redox potentials of the nanocrystals. Here we discuss the results of recent systematic electrochemical investigations aimed at understanding the structural factors that regulate the redox properties of CdSe core and CdSe–ZnS core–shell QDs.

Keywords: electrochemistry; electron transfer; nanoparticles; redox potentials; voltammetry.

INTRODUCTION

Semiconductor quantum dots

Semiconductor quantum dots (QDs) are nanoscaled inorganic crystals characterized by very interesting optical and electronic properties [1]. Noticeably, they exhibit an intense luminescence with a narrow emission band that can be carefully positioned across the visible and near-infrared spectral regions by regulating their elemental composition and physical dimensions. Their huge molar extinction coefficients across the UV–vis region permit luminescence measurements in conditions of extreme dilution and low excitation power. The large two-photon absorption cross-section renders QDs interesting dyes for applications where biphotonic excitation is required (e.g., biological imaging). In short, these nanocrystals constitute a promising alternative to molecular dyes for a variety of applications [2], spanning analytical sciences (e.g., luminescent sensors), diagnostics (e.g., fluorescence microscopy imaging), and materials science (e.g., materials for light-emitting devices, additives for polymers). The high interest in QDs is witnessed by the very rapid growth of the number of research papers, reviews [3], and books [4] dealing with such nanomaterials since their discovery in the early 1980s and the development of preparation methods based on wet chemical reactions [5].

Pure Appl. Chem.* **83, 1–252 (2011). A collection of invited, peer-reviewed articles by former winners of the IUPAC Prize for Young Chemists, in celebration of the International Year of Chemistry 2011.
‡Corresponding author

QDs are generally prepared by reacting inorganic precursors in the presence of organic ligands, which eventually form a molecular coating around the QD luminescent core and stabilize the nanoparticles against aggregation. Chemical modification of this coating allows the regulation of the physicochemical properties of QDs in order to, e.g., confer solubility in water (useful for biological applications) or protect the luminescent emission from external quenchers. Moreover, the luminescent core of QDs can be passivated with protective inorganic shells to improve the emission efficiency and the photobleaching resistance.

One of the major research themes in the past two decades has been the design and construction of molecular devices, that is, ordered assemblies of molecular components conceived to perform a specific task [6]. As a matter of fact, photoinduced electron transfer has emerged as a versatile mechanism to implement light-induced functionalities in multicomponent (supra)molecular assemblies [7]. This research has led to the construction of, e.g., molecule-based wires, switches, sensors, logic gates, and mechanical machines [6]. Because of their valuable physicochemical properties, QDs are most appealing candidates to play the role of active components in new generations of photochemical molecular devices [3,8,9].

Electrochemical investigations of quantum dots

The rational design of molecular devices based on electron transfer (be it photoinduced or not) requires prior knowledge of the redox potentials of the components. The fine-tuning of these parameters, together with the structural and geometric characteristic of the connection between the components, is essential to achieve the desired function [7]. In this context, the large amount of information available on the structural and electronic properties of molecular species is invaluable for the development of functional assemblies [10]. In contrast, the same level of understanding on the interplay between the structural and electronic properties of QDs has not yet been achieved. Particularly, the influence of the diameter of their luminescent core, thickness of their protecting shell (if any), and nature of the passivating ligands on their redox potentials is still rather unclear. In fact, specific investigations of the relationship between the structure and the redox properties of QDs are rare [11]. Here we discuss the results of recent systematic electrochemical studies aimed at understanding the structural factors that regulate the redox properties of CdSe core and CdSe–ZnS core–shell QDs.

Electrochemical measurements of QDs can, in principle, give information on the absolute energies of the valence and conduction bands (from the redox potential values) and on the rate constants of the heterogeneous electron-transfer processes involving the nanocrystal. Electrochemical experiments on QDs in solution, however, are not trivial because the low solubility and the small diffusion coefficients of the particles result in current intensities that are difficult to measure against the background signal [12]. For this reason, voltammetric techniques that suppress the background current, such as square wave voltammetry (SWV) and differential pulse voltammetry (DPV), are often used for the identification of the redox processes and the determination of the corresponding potential values. Another possibility is to perform voltammetric measurements on QD samples adsorbed on the working electrode [13]. The reversibility of the redox processes is usually assessed by cyclic voltammetry (CV).

The electrochemical bandgap energy ΔE_{el}, calculated from the difference between the potentials for oxidation and reduction of the QD, can be related to the optical bandgap energy ΔE_{op}, determined from spectroscopic measurements, by eq. 1 [14]:

$$\Delta E_{op} = \Delta E_{el} - J_{e-h} \quad (1)$$

in which J_{e-h} is the total Coulomb energy of the electron-hole pair. Hence, for any given QD, ΔE_{el} is expected to be larger than ΔE_{op} [14].

RESULTS AND DISCUSSION

CdSe core nanocrystals

A series of CdSe QDs with three different diameters (**a1**–**a3**) were synthesized and their voltammetric behavior in tetrahydrofuran (THF) solution was investigated [15]. The nanocrystals were prepared by the so-called hot injection method [4] using tris-*n*-octylphosphine oxide (TOPO) as both the solvent and the surfactant; the surface-adsorbed TOPO molecules were subsequently exchanged with *n*-decanethiol ligands. The electrochemical properties of these samples, together with the optical bandgap, are gathered in Table 1. Figure 1 shows the DPV scans for oxidation of these QDs.

Table 1 Redox potentials, and electrochemical and optical bandgaps of *n*-decanethiol-coated CdSe QDs with different core diameters (THF, room temperature).

Sample	d_{core} (nm)[a]	E_{ox} (V)[b]	E_{red} (V)[b]	ΔE_{el} (V)[c]	ΔE_{op} (V)[d]
a1	2.1	+1.16	–1.07	2.24	2.66
a2	2.3	+0.82	–1.20	2.03	2.53
a3	2.5	+0.68	–1.26	1.94	2.41

[a]Mean core diameter, determined from optical measurements [16].
[b]Potential values for the first oxidation and reduction of the QDs, referred to the Ag/AgCl (3 M KCl) electrode; glassy carbon working electrode, tetrabutylammonium hexafluorophosphate 0.1 M as supporting electrolyte.
[c]Electrochemical bandgap, determined from the difference between E_{ox} and E_{red}.
[d]Optical bandgap, determined from the onset of the lowest energy absorption band.

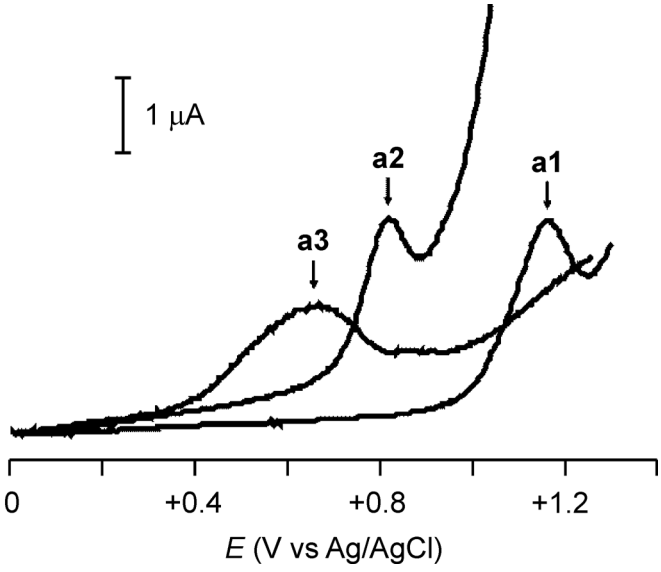

Fig. 1 DPV pattern for the oxidation of *n*-decanethiol-coated CdSe QDs **a1**, **a2**, and **a3**, possessing core diameters of 2.1, 2.3, and 2.5 nm, respectively. Conditions: 1.5 μM, THF/0.1 M Bu_4NPF_6, glassy carbon working electrode, 20 mV s^{-1}, room temperature.

The voltammetric scans for each of the **a1**–**a3** QDs in the examined potential window show one irreversible oxidation (Fig. 1) and one irreversible reduction process. The potentials for the oxidation and reduction of the QDs (E_{ox} and E_{red} in Table 1) shift in the negative direction with an increase in core diameter. The chemical irreversibility of these processes can be explained considering that the addition or removal of electrons to/from the nanoparticle may be followed by decomposition reactions (e.g., detachment of Cd or Se atoms). The electrochemical bandgap energy (ΔE_{el} in Table 1) decreases with an increase in core diameter, in agreement with previous experimental observations [11] and theoretical calculations [14]. This trend parallels that of the optical bandgap energy (ΔE_{op} in Table 1). It should be noted, however, that the electrochemical bandgap energy is 0.4–0.5 eV smaller than the optical counterpart in all instances, in contrast with expectations (see above). A reason for this discrepancy may be the fact that, because electrochemical experiments probe surface levels, ΔE_{el} is affected by the presence of surface defects [4] that act as local trap states for electrons and holes [12,17]. Such an interpretation is, in fact, supported by the observation of a tail in the emission bands of this set of CdSe QDs [15]. Another possibility is that the bandgap energy determined electrochemically is underestimated because of the chemical reactions that follow the redox processes.

In order to probe the influence of the procedure adopted for the synthesis of the QDs on their redox properties, we synthesized another series of CdSe nanocrystals with four different core diameters (**b1**–**b4**) following a slightly different protocol [18]. The hot injection method was again used but octadecene was employed as a non-coordinating solvent, and TOPO and hexadecylamine (HDA) played the role of the surface ligands. Table 2 lists the electrochemical properties and the optical bandgap of these QDs in chloroform solution. The DPV reduction scans displayed in Figure 2 show the typical voltammetric response of these species.

Table 2 Redox potentials, and electrochemical and optical bandgaps of TOPO/HDA-coated CdSe QDs with different core diameters ($CHCl_3$, room temperature).

Sample	d_{core} (nm)[a]	E_{ox} (V)[b]	E_{red} (V)[b]	ΔE_{el} (V)[c]	ΔE_{op} (V)[d]
b1	2.6	+1.10	–0.99	2.09	2.30
b2	3.1	+1.79	–1.21	3.00	2.18
b3	3.8	+1.77	–1.25	3.02	2.09
b4	4.3	+1.02	–0.89	1.91	2.04

[a]Mean core diameter, determined from transmission electron microscopy and optical measurements [16].
[b]Potential values for the first oxidation and reduction of the QDs, referred to the Ag/AgCl (3 M KCl) electrode; glassy carbon working electrode, tetrabutylammonium hexafluorophosphate 0.1 M as supporting electrolyte.
[c]Electrochemical bandgap, determined from the difference between E_{ox} and E_{red}.
[d]Optical bandgap, determined from the onset of the lowest energy absorption band.

Contrary to what was observed for the previous series [15], the redox potentials are not monotonously related to the QD size. Specifically, the electrochemical bandgap increases with increasing the diameter for samples **b1**, **b2**, and **b3**, in contrast with the expected behavior that is reflected by the optical bandgap. Moreover, ΔE_{el} is larger than ΔE_{op} (as expected from eq. 1) only for QDs **b2** and **b3**, whereas for **b1** and **b4** ΔE_{el} results to be smaller than ΔE_{op}. In fact, the small nanocrystals **b1** are both easier to oxidize and to reduce than larger particles **b3**.

These results indicate that, while the optical bandgap depends on the actual electron-hole recombination within the nanocrystal and therefore follows the size dependence expected from the particle-in-a-box model, the electrochemical processes of these QDs are strongly affected by other factors. As noted above, it is likely that surface defects play a major role in determining the redox potentials. Our experiments suggest that the influence of these defects on the potential values is dominant for the small-

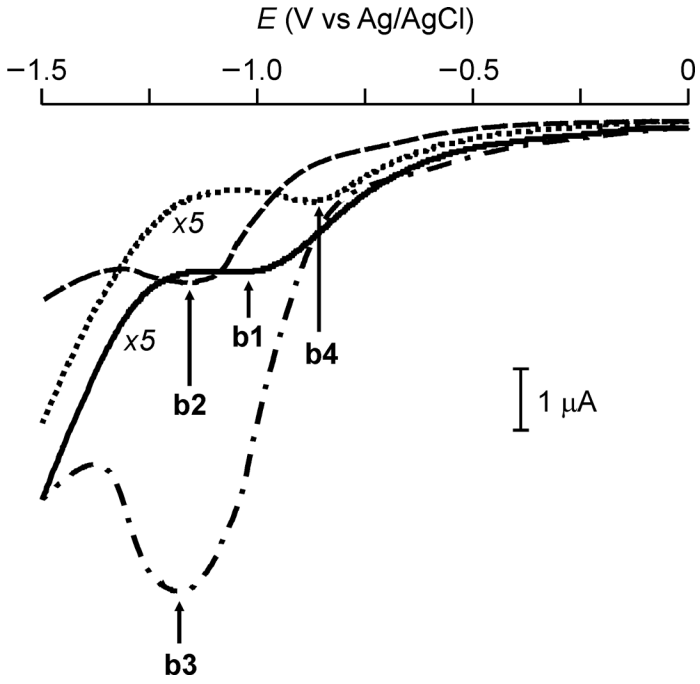

Fig. 2 DPV pattern for the reduction of TOPO/HDA-coated CdSe QDs **b1** (——), **b2** (– – –), **b3** (– · – ·), and **b4** (· · · · ·), possessing core diameters of 2.6, 3.1, 3.8, and 4.3 nm, respectively. Conditions: 5 μM, $CHCl_3$/0.1 M Bu_4NPF_6, glassy carbon working electrode, 20 mV s^{-1}, room temperature.

est and the largest particles of our series, while for mid-sized QDs the electrochemical bandgap is consistent with the optical bandgap. Such observations are confirmed by a closer inspection of the respective luminescence bands and quantum yields, which can be used to monitor the extent of surface defects [18].

A possible explanation for this behavior is that small particles have more defects [19] because of the relatively short reaction time, which does not allow thermal annealing. Mid-sized particles, growing in the focusing regime [4,20], most likely experience a correction of surface defects besides the narrowing of the size distribution. The growth of larger particles can occur, at least in part, by Ostwald ripening (disassembly of small crystals and incorporation of the resulting material into larger ones). Therefore, the building blocks reacting on the surface in this regime derive from small QDs which, as noted above, carry a substantial amount of defects.

CdSe–ZnS core–shell nanocrystals

An efficient strategy to control and improve the physicochemical (in particular, optical) properties of QDs is to grow a shell of a second semiconductor on the top of the nanocrystal core [21]. Such an inorganic shell removes the discontinuity represented by the core–ligand interface, thus partially eliminating surface defects, and protects the core from the interaction with the environment. CdSe–ZnS core–shell systems represent the most common choice because these QDs are strongly emissive in the visible region.

We synthesized a series of QDs with the same CdSe core diameter and ZnS shells of different thicnkess (**c1**–**c3**) to investigate the influence of the shell thickness on the redox properties of the nanocrystals [15]. Similarly to the **a1**–**a3** series, the native TOPO ligands were replaced with

n-decanethiol ligands. The electrochemical properties and the optical bandgap of these samples are gathered in Table 3. The voltammetric response of these nanocrystals is qualitatively similar to that of the previously discussed series.

Table 3 Redox potentials, and electrochemical and optical bandgaps of *n*-decanethiol-coated CdSe–ZnS QDs with core diameter of 2.2 nm and different shell thickness (THF, room temperature).

Sample	t_{shell} (nm)[a]	E_{ox} (V)[b]	E_{red} (V)[b]	ΔE_{el} (V)[c]	ΔE_{op} (V)[d]
c1	1.4	+1.56	–0.98	2.53	2.56
c2	2.2	+1.45	–1.00	2.45	2.55
c3	5.0	+1.25	–1.12	2.37	2.53

[a]Shell thickness, determined by subtracting the core diameter (estimated from optical measurements according to ref. [16]) from the core–shell diameter measured by transmission electron microscopy.
[b]Potential values for the first oxidation and reduction of the QDs, referred to the Ag/AgCl (3 M KCl) electrode; glassy carbon working electrode, tetrabutylammonium hexafluorophosphate 0.1 M as supporting electrolyte.
[c]Electrochemical bandgap, determined from the difference between E_{ox} and E_{red}.
[d]Optical bandgap, determined from the onset of the lowest energy absorption band.

The voltammetric scans for each of the **c1**–**c3** QDs in the examined potential window show one irreversible oxidation and one irreversible reduction process. The addition of a ZnS shell around the CdSe core shifts both redox potentials in the positive direction. The shell significantly hampers oxidation but slightly facilitates reduction, while having negligible influence on ΔE_{op} (Tables 1 and 3). The positive potential shift of the oxidative process is in qualitative agreement with the change in the valence band energy on going from CdSe to ZnS [21], suggesting that the oxidation of the CdSe–ZnS nanoparticles may involve the removal of electrons from the inorganic shell. However, the significant increase of the luminescence quantum yield upon deposition of the ZnS layer indicates that the electrochemical response of the nanoparticles is most likely dominated by surface states. Presumably, dangling electrons on the CdSe surface are responsible for oxidation in the absence of a ZnS shell, and their passivation results in the observed potential shift with a concomitant enhancement in luminescence quantum yield (vide supra). Furthermore, an increase in shell thickness translates into a shift of both potentials in the negative direction. This trend is qualitatively similar to that observed upon increasing the CdSe core diameter (Table 1). Similarly, the electrochemical bandgap decreases with an increase in shell thickness. By contrast, the shell thickness has a negligible influence on the optical bandgap. Hence, the ZnS shell affects substantially the electrochemical response of these nanoparticles, while having a modest effect on their visible absorption spectrum.

CONCLUSION

We have studied the electrochemical behavior of families of CdSe and CdSe–ZnS core–shell QDs in order to investigate the influence of the structural parameters (specifically, the diameter of the core and the thickness of the shell) and the synthetic procedure on the redox potentials of these semiconductor nanocrystals. Our results have shown that the potentials for the oxidation and reduction of the QDs depend on the core diameter and, in the case of the core–shell nanocrystals, also on the shell thickness. The electrochemical bandgap is found to be inversely proportional to the core diameter (as expected from the particle-in-a-box model) only for the QDs in which the TOPO molecules, employed as both the solvent and the surfactant, are successively replaced with *n*-decanethiol ligands (**a1**–**a3**). The electrochemical bandgap is, however, somewhat smaller than the optical bandgap, suggesting the participation of surface defects in the redox processes.

In the case of CdSe QDs prepared using octadecene as a non-coordinating solvent, and TOPO and HDA as surfactants (**b1**–**b4**), we observed that the redox potentials are not monotonously related to the QD size, in contrast with what was observed for samples **a1**–**a3**. Specifically, the electrochemical bandgap values are consistent with those of the optical bandgap only for the mid-sized QDs **b2** and **b3**. Again, it is likely that the redox properties of the QDs are dominated by surface traps for electrons and holes. An explanation for the observed behavior can be attempted by estimating the extent of surface defects in these QDs, on the basis of the processes that are important to the synthesis of small, mid-sized, and large nanocrystals.

The addition of a ZnS shell around the CdSe core shifts both potentials in the positive direction (compare, e.g., **a2** with **c1**–**c3**). The shell thickness has a significant influence on the electrochemical bandgap, but essentially no effect on the optical counterpart, indicating, once again, that surface defects participate in the redox processes.

In summary, our results show that the potentials for oxidation and reduction of CdSe-type semiconductor nanocrystals can be determined by pulse voltammetric measurements in solution. These values, however, reflect the position of the conduction and valence bands edges only for nanocrystals possessing a relatively small number of surface defects. Such considerations have to be taken into account in the design and preparation of nanoscale devices that employ QDs as components involved in electron-transfer processes. Examples of this kind of device are luminescent sensors that use photoinduced electron transfer from/to a QD as the mechanism to switch on/off the nanocrystal emission [3,8,9].

ACKNOWLEDGMENTS

Financial support from MIUR (PRIN 2008), MAE (DGPCC), Università di Bologna, Fondazione Carisbo, the U.S. National Science Foundation (CAREER Award CHE-0237578 and CHE-0749840), and the University of Miami is gratefully acknowledged.

REFERENCES

1. (a) M. G. Bawendi, M. L. Steigerwald, L. E. Brus. *Ann. Rev. Phys. Chem.* **41**, 477 (1990); (b) A. P. Alivisatos. *Science* **271**, 933 (1996); (c) A. L. Efros, M. Rosen. *Ann. Rev. Mater. Sci.* **30**, 475 (2000).
2. (a) X. Michalet, F. F. Pinaud, L. A. Bentolila, J. M. Tsay, S. Doose, J. J. Li, G. Sundaresan, A. M. Wu, S. S. Gambhir, S. Weiss. *Science* **307**, 538 (2005); (b) U. Resch-Genger, M. Grabolle, S. Cavaliere-Jaricot, R. Nitschke, T. Nann. *Nat. Meth.* **5**, 763 (2008).
3. See, e.g.: (a) R. C. Somers, M. G. Bawendi, D. G. Nocera. *Chem. Soc. Rev.* **36**, 579 (2007); (b) I. Yildiz, E. Deniz, F. M. Raymo. *Chem. Soc. Rev.* **38**, 1859 (2009); (c) D. V. Talapin, J. S. Lee, M. V. Kovalenko, E. V. Shevchenko. *Chem. Rev.* **110**, 389 (2010); (d) A. M. Smith, S. Nie. *Acc. Chem. Res.* **43**, 190 (2010).
4. A. L. Rogach (Ed.). *Semiconductor Nanocrystal Quantum Dots*, Springer-Verlag, Vienna (2008).
5. C. B. Murray, D. J. Norris, M. G. Bawendi. *J. Am. Chem. Soc.* **115**, 8706 (1993).
6. V. Balzani, A. Credi, M. Venturi. *Molecular Devices and Machines—Concepts and Perspectives for the Nano World*, Wiley-VCH, Weinheim (2008).
7. (a) A. P. de Silva, H. Q. N. Gunaratne, T. Gunnlaugsson, A. J. M. Huxley, C. P. McCoy, J. T. Rademacher, T. E. Rice. *Chem. Rev.* **97**, 1515 (1997); (b) R. Ballardini, A. Credi, M. T. Gandolfi, F. Marchioni, S. Silvi, M. Venturi. *Photochem. Photobiol. Sci.* **6**, 345 (2007).
8. (a) B. Gadenne, I. Yildiz, M. Amelia, F. Ciesa, A. Secchi, A. Arduini, A. Credi, F. M. Raymo. *J. Mater. Chem.* **18**, 2022 (2008); (b) M. Amelia, A. Lavie-Cambot, N. D. McClenaghan, A. Credi. *Chem. Commun.* In press.

9. Recent examples: (a) E. J. McLaurin, A. B. Greytak, M. G. Bawendi, D. G. Nocera. *J. Am. Chem. Soc.* **131**, 12994 (2009); (b) I. L. Medintz, T. Pons, K. Susumu, K. Boeneman, A. M. Dennis, D. Farrell, J. R. Deschamps, J. S. Melinger, G. Bao, H. Mattoussi. *J. Phys. Chem. C* **113**, 18552 (2009); (c) R. C. Mulrooney, N. Singh, N. Kaur, J. F. Callan. *Chem. Commun.* 686 (2009); (d) D. Geissler, L. J. Charbonniere, R. F. Ziessel, N. G. Butlin, H.-G. Lohmannsroben, N. Hildebrandt. *Angew. Chem., Int. Ed.* **49**, 1396 (2010); (e) Z. Erno, I. Yildiz, B. Gorodetsky, F. M. Raymo, N. R. Branda. *Photochem. Photobiol. Sci.* **9**, 249 (2010); (f) M. Amelia, R. Flamini, L. Latterini. *Langmuir* **26**, 10129 (2010).
10. P. Ceroni, A. Credi, M. Venturi (Eds.). *Electrochemistry of Functional Supramolecular Systems*, John Wiley, New York (2010).
11. (a) S. K. Haram, B. M. Quinn, A. J. Bard. *J. Am. Chem. Soc.* **123**, 8860 (2001); (b) C. Querner, P. Reiss, S. Sadki, M. Zagorska, A. Pron. *Phys. Chem. Chem. Phys.* **7**, 3204 (2005); (c) E. Kuçur, W. Bücking, S. Arenz, R. Giernoth, T. Nann. *ChemPhysChem* **7**, 77 (2006).
12. A. J. Bard, Z. Ding, N. Myung. *Struct. Bond.* **118**, 1 (2005).
13. E. Kuçur, J. Riegler, G. A. Urban, T. Nann. *J. Chem. Phys.* **119**, 2333 (2003).
14. A. Franceschetti, A. Zunger. *Appl. Phys. Lett.* **76**, 1731 (2000).
15. S. Impellizzeri, S. Monaco, I. Yildiz, M. Amelia, A. Credi, F. M. Raymo. *J. Phys. Chem. C* **114**, 7007 (2010).
16. W. Yu, L. Qu, W. Guo, X. Peng. *Chem. Mater.* **15**, 2854 (2003).
17. E. Kuçur, W. Bücking, T. Nann. *Microchim. Acta* **160**, 299 (2008).
18. M. Amelia, S. Monaco, S. Impellizzeri, I. Yildiz, F. M. Raymo, A. Credi. Manuscript in preparation.
19. D. Pan, Q. Wang, S. Jiang, X. Li, L. An. *Adv. Mater.* **17**, 176 (2005).
20. (a) T. Sugimoto. *Adv. Colloid Interface Sci.* **28**, 65 (1987); (b) X. Peng, J. Wickham, A. P. Alivisatos. *J. Am. Chem. Soc*. **120**, 5343 (1998).
21. P. Reiss, M. Protière, L. Li. *Small* **5**, 154 (2009).

